Speciation of "brown" carbon in cloud water impacted by agricultural biomass burning in eastern China

Yury Desyaterik,[1] Yele Sun,[1,2] Xinhua Shen,[1,3] Taehyoung Lee,[1,4] Xinfeng Wang,[5,6] Tao Wang,[5,6] and Jeffrey L. Collett Jr.[1]

Received 12 February 2013; revised 31 May 2013; accepted 5 June 2013.

[1] Despite growing interest in the visible light-absorbing organic component of atmospheric aerosols, referred to as "brown" carbon, our knowledge of its chemical composition remains limited. It is well accepted that biomass burning is one important source of "brown" carbon in the atmosphere. In this study, cloud water samples heavily affected by biomass burning were collected at Mount Tai (1534 m, ASL), located in Shandong province in the North China Plain in summer 2008. The samples were analyzed with high performance liquid chromatography equipped with a UV/Vis absorbance detector immediately followed by electrospray ionization and analysis using a time-of-flight (ToF) mass spectrometer. The high mass resolution and accuracy provided by the ToF mass spectrometer allow determination of the elemental composition of detected ions. Using this approach, the elemental compositions of 16 major light-absorbing compounds, which together accounted for approximately half of measured sample absorption between 300 and 400 nm, were determined. The most important classes of light-absorbing compounds were found to be nitrophenols and aromatic carbonyls. Light absorption over this wavelength range by reduced nitrogen compounds was insignificant in these samples.

Citation: Desyaterik, Y., Y. Sun, X. Shen, T. Lee, X. Wang, T. Wang, and J. L. Collett Jr. (2013), Speciation of "brown" carbon in cloud water impacted by agricultural biomass burning in eastern China, *J. Geophys. Res. Atmos.*, *118*, doi:10.1002/jgrd.50561.

1. Introduction

[2] Interaction of atmospheric aerosols with solar radiation is an important factor influencing climate forcing. Airborne particles can backscatter incoming solar radiation, cooling the atmosphere, while some particle types also can absorb solar radiation and heat the atmosphere. The most effective absorber of solar radiation is black carbon (BC) [*Hansen et al*., 1984; *Penner et al*., 1993]. BC is formed by incomplete combustion of carbonaceous fuels and consists of mostly elemental carbon in several linked forms [*Cooke et al*., 1999]. Because of its significant effects on radiative transfer and climate, BC has been intensively studied [e.g., *Chuang et al*., 2003; *Bond and Bergstrom*, 2006; *Ramanathan and Carmichael*, 2008].

[3] Several studies have found that certain fractions of organic aerosols also absorb solar radiation effectively, but differently from blank carbon. The difference is in the spectral dependence of absorption. Certain organic compounds absorb strongly in the UV and short wavelength visible region of the spectrum [*Andreae and Gelencsér*, 2006; *Moosmüller et al*., 2009]. Because of this optical property, they appear to have a brownish or yellowish color. The term "Brown Carbon" (BrC) was suggested [*Formenti et al*., 2003] for colored organic compounds in pyrogenic aerosols. The wavelength dependence of aerosol absorption is usually parameterized by an empirical relationship as proportional to $\lambda^{-Å}$, where λ is the wavelength of light, and Å is the absorption Angstrom exponent (AAE). This parameter is not fundamental and for aerosols depends not only on properties of bulk matter, but also on particle morphology and size [*Moosmüller et al*., 2011]. For BC, the value of the Angstrom exponent is close to 1 [*Bergstrom et al*., 2002; *Schnaiter et al*., 2003; *Kirchstetter et al*., 2004]. Aerosols with AAE values of 2 and higher have been found in fresh smoke, at rural locations and in urban conditions. AAE values between 6 and 7 were found for humic-like substance (HULIS) extracted from aerosols collected in Brazil during the most active biomass burning period in this region [*Hoffer et al*., 2006]. For the organic carbon component of

[1]Department of Atmospheric Science, Colorado State University, Fort Collins, Colorado, USA.
[2]State Key Laboratory of Atmospheric Boundary Layer Physics and Atmospheric Chemistry, Institute of Atmospheric Physics, Chinese Academy of Sciences, Beijing, China.
[3]Now at Department of Civil and Environmental Engineering, Prairie View A&M University, Prairie View, Texas, USA.
[4]Now at Department of Environmental Science, Hankuk University of Foreign Studies, Seoul, South Korea.
[5]Department of Civil and Environmental Engineering, The Hong Kong Polytechnic University, Kowloon, Hong Kong.
[6]Environment Research Institute, Shandong University, Jinan, China.

Corresponding author: Y. Desyaterik, Department of Atmospheric Science, Colorado State University, Campus delivery 1731, Fort Collins, CO 80523 USA. (desyater@engr.colostate.edu)

2169-897X/13/10.1002/jgrd.50561

aerosols in the Mexico City metropolitan area, AAE was found to be 2.4 on average and as high as 5.1 at some times [*Barnard et al*., 2008]. AAE values of carbonaceous particles measured since *Kirchstetter et al*. [2004] have been summarized [*Bergstrom et al*., 2007], and values higher than 2 were consistently found for biomass combustion smoke. In the recent CalNex campaign, the water-soluble organic carbon (WSOC) fraction of $PM_{2.5}$ aerosols from Los Angeles was analyzed with a spectrophotometer [*Zhang et al*., 2011, 2013]. AAE was found to be in a range from 1.2 to 5.4 with a mean value of 3.2 for wavelengths between 300 and 600 nm. Eight nitrogen-containing mono- and polyaromatic compounds that absorb light at 365 nm were quantified. It was estimated that these compounds contributed approximately 4% of the total WSOC absorption at 365 nm. In addition, the authors found that when methanol was used for filter extraction, the samples show higher absorption than observed for aqueous extracts. In recent smog chamber studies [*Jaoui et al*., 2008; *Zhong and Jang*, 2011], organic aerosols produced by photo-oxidation of toluene, the most abundant aromatic compound in urban air [*Kelly et al*., 2010], were analyzed. The main nitrogen-containing compounds were found to be isomers of 2-hydroxy-5-nitrobenzyl alcohol, an observation supported by detailed kinetic modeling of toluene oxidation [*Kelly et al*., 2010]. A similar compound, $C_7H_7NO_4$, was also found in the CalNex study [*Zhang et al*., 2011, 2013], but the correlation between its concentration and total light absorption at 365 nm was low ($r^2 = 0.38$). Winter and summer aerosol samples from an urban location in Ljubljana, Slovenia, were analyzed and 12 nitro-aromatic compounds were quantified [*Kitanovski et al*., 2012b]. In winter aerosols, nitro-aromatics constituted a non-negligible fraction of the OC: 0.8%, on average, with the highest contributions from 4-nitrocatechol (4NC) and methyl-nitrocatechols. Much higher winter concentrations of nitro-aromatics, for example, the 4NC concentration was 310 times higher in winter than in summer, were ascribed to biomass burning activities and confirmed by high concentrations of levoglucosan in winter samples. 4NC was also found to be the major component of HULIS extracted from $PM_{2.5}$ samples obtained from Budapest and K-puszta, Hungary, and Rondonia, Brazil [*Claeys et al*., 2012]. The highest concentration of 4NC was found in Brazil samples affected by BB. For biogenic aerosols measured over the Amazon Basin, AAE was observed in a range from 1.3 to 1.9 with the lowest value during dry season [*Rizzo et al*., 2011]. For carbon spheres collected in East Asian outflow, AAE was estimated to be 1.5 from measurements of electron energy losses from individual spheres [*Alexander et al*., 2008]. Similar spherical carbonaceous particles—"tar balls"—from smoldering combustion of two fuels Ponderosa Pine and Alaskan Duff were found in laboratory experiments [*Chakrabarty et al*., 2010]. AAE for these particles was found to range between 4.2 and 6.4 measured at 405–532 nm. AAE was measured for smoke from 14 different fuels with a dual-wavelength photoacoustic instrument operating at 405 and 870 nm [*Lewis et al*., 2008]. Values close to 1 were found for fuels when the organic fraction of the smoke was considerably less than the elemental carbon fraction. Values as high as 3.5 were associated with light-absorbing organic material present in a wood smoke. In another study, AAE was measured for methanol and water filter extracts from aerosols generated by wood pyrolysis [*Chen and Bond*, 2010]. Interestingly, a large fraction of the absorbing part was water insoluble, but extractable by methanol. AAE values found for methanol extract were in the range 7–12. Biomass burning and pollution plumes identified from trace gas measurements were evaluated for their aerosol optical signatures during extensive flights over North America for the INTEX/ICARTT experiment in summer 2004 [*Clarke et al*., 2007]. The AAE (470–660 nm) for BB plumes had a value centered about 2.1, while that of pollution plumes was lower, often near 1. Light absorption of aqueous extracts from filters from 15 southeastern US monitoring sites over the year 2007 were reported, as well as online measurements from a Particle-Into-Liquid Sampler deployed from July to mid-August 2009 in Atlanta, Georgia. Three main sources of soluble chromophores were identified: biomass burning, mobile source emissions, and compounds linked to secondary organic aerosol (SOA) formation. Angstrom exponents were around 7 for biomass burning and nonbiomass burning-impacted filter samples [*Hecobian et al*., 2010]. The amount of light-absorbing organic carbon was estimated from AERONET measurements. Relatively high columnar absorbing levels of BrC were found in biomass burning regions of South America and Africa (about 15–20 mg/m^2 during biomass burning seasons), while the concentrations were significantly lower in urban areas in the US and Europe [*Arola et al*., 2011]. A significant amount of absorbing organic carbon was found from observations in megacities, particularly in India and China, with peak values up to 30–35 mg/m^2 during the coldest season, likely caused by emissions from coal and biofuel burning used for heating. Biomass burning, including domestic wood burning in winter and agricultural fires in spring, was identified as a major source of BrC at six sites across Europe [*Lukács et al*., 2007]. Overall, this body of literature indicates that high AAE coefficients are often associated with biomass burning.

[4] Differences between the optical properties of BC and BrC are related to differing chemical properties. BC has a graphite-like microcrystalline structure, as evident from Raman spectroscopy [*Rosen and Novakov*, 1977]. In graphitic structures, there are many carbon atoms connected by π bonds, creating delocalized electrons. These electrons are able to absorb light in a broad range of wavelengths from infrared to ultraviolet. Because they collectively absorb all wavelengths of visible light, the material appears black in color. Organic carbon found in atmospheric aerosols usually does not contain large numbers of molecules with extended conjugated π-electron systems, because double bonds quickly react with ozone. Molecules with aromatic moieties are more stable; however, having one benzene ring does not provide absorption in the UVA or visible range. Molecules that absorb in the UVA/visible range may either have a few fused aromatic rings (polyaromatic hydrocarbons) or have additional heteroatoms, O or N, attached to a single aromatic ring such as a carbonyl or nitro group. Heteroatoms allow for an n-π^* transition, which reduces the electronic transition energy to a range corresponding to the energy of photons in the shorter visible wavelength range. The selective absorbance of shorter visible wavelengths removes the violet/blue part of the spectrum leaving the material with a yellow-to-brown appearance.

a)  b) 

Figure 1. (a) Photograph of unfiltered cloud water samples collected at Mt. Tai on 19 June 2008. From left to right, the three bottles contain bulk, large drop, and small drop samples, respectively, (b) Photograph of filtered cloud water samples from the same date.

[5] The role of BrC as an absorber of solar radiation was recently reviewed by *Feng et al.* [2013]. Inclusion of BrC in global simulations alters the calculated direct radiative effect of organic carbonaceous aerosols from net cooling ($-0.08\ W\ m^{-2}$) to warming ($+0.025\ W\ m^{-2}$) at the top of the atmosphere. Influence of BrC over source regions and above clouds is more substantial and may affect the hydrologic cycle. Since absorption of BrC is mainly in the UV, it may affect the ultraviolet actinic flux and thus photochemistry.

[6] As for the chemical nature of BrC, it has been suggested that it may include humic substances, polyaromatic hydrocarbons, and lignin [*Andreae and Gelencsér*, 2006]. The possible importance of nitrated and aromatic aerosol components for near UV light absorption has also been suggested [*Jacobson*, 1999]. A number of laboratory studies reported the formation of colored organic matter in the reaction of glyoxal in ammonium sulfate and ammonium nitrate solution [*Shapiro et al*., 2009], oxidation of phenol in a solution of hydrogen peroxide [*Chang and Thompson*, 2010], and reaction of SOA produced by limonene ozonolysis with ammonia [*Bones et al*., 2010]. Although fog and cloud samples have sometimes been observed to exhibit a yellowish color [e.g., *Collett et al*., 1999], the composition of light-absorbing organics in cloud water has not been reported, to the best of our knowledge.

[7] In this study, we determine the composition of organic matter in cloud water impacted by agricultural biomass burning. The presence of substantial amounts of BrC was obvious from the yellowish appearance of the cloud water. Filtered and unfiltered sample photographs are shown in Figures 1a and 1b. Liquid chromatography coupled with detection by UV/Vis absorbance and mass spectrometry is applied to determine the composition of the most important light-absorbing compounds in the cloud water.

2. Methods

2.1. Sample Collection

[8] Cloud water samples were collected at the summit of Mt. Tai (36.251°N, 117.101°E, 1534 m, asl), located in Shandong province in the North China Plain, in the summer (14 June – 16 July) of 2008 using a Caltech Active Strand Cloudwater Collector (CASCC) [*Demoz et al*., 1996]. A two-stage size-fractionating CASCC (sf-CASCC, the 50% lower drop size cutoff for the first and second stages is approximately 16 and 4 μm diameter) was also used to simultaneously collect small and large cloud drop samples. The cloud collectors were cleaned prior to each cloud interception event using high purity deionized water. Collocated measurements include monitoring of cloud liquid water content (LWC) using a Particulate Volume Monitor (Gerber Scientific, model PVM-100), and collection of interstitial aerosol particles and gas-phase species (HNO_3, NH_3, and SO_2) using a University Research Glassware denuder and filter pack assembly. Detailed descriptions of the sampling site and field measurements are given by *Shen et al*. [2012].

2.2. Chemical Analyses

[9] Immediate analyses after sample collection included measurement of sample weight and pH measurement with an Orion portable pH meter (model 290A). All sample aliquots were refrigerated on-site and were express shipped cold to Colorado State University. The samples were kept frozen in the dark prior to the analysis. Routine sample analysis included measurements of major anions (SO_4^{2-}, NO_3^-, Cl^-, and NO_2^-) and cations (Na^+, NH_4^+, K^+, Mg^{2+}, and Ca^{2+}) by two ion chromatography (DIONEX DX-500) systems and analysis of total organic carbon (TOC) by a Shimadzu TOC Analyzer (model: TOC – V_{CSH}). Additional analysis of collected samples, including measurement of H_2O_2, HCHO, S(IV), Fe, and Mn concentrations in the cloud samples, was also completed as described by *Shen et al*. [2012].

[10] Cloud samples were filtered using disposable syringe filters (Puradisc 25 TF, PTFE membrane with 0.2 μm pore size) and directly analyzed without any preconcentration for organic constituents with an Agilent 1100 Series liquid chromatograph coupled to a UV/Vis diode array detector (Agilent G1315D) followed by a time-of-flight mass spectrometer (Agilent LC/MCD TOF G1969A) with an electrospray ionization source. LC/DAD-ESI-HR-TOFMS analysis was performed in February 2011. The absorbance detector monitored absorbance from 190 to 900 nm with a data capture rate of 2 Hz. The ToF-MS was operated in both negative and positive ion modes. Mass accuracy and mass resolution for the detector were approximately 5 ppm and 4000–7000, respectively, for singly charged masses in the range of 100 to 300 Da. The MS signal was acquired at 1.4 Hz. The combination of a diode array detector with the ToF-MS means that both compound absorbance and mass can be obtained across a wide range simultaneously without

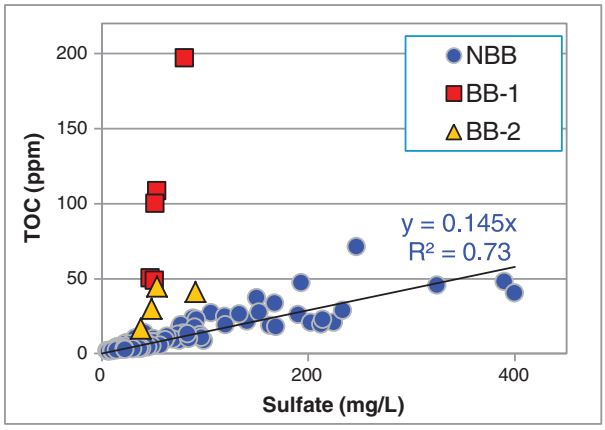

Figure 2. Correlations between TOC and sulfate concentrations in Mt. Tai summer bulk cloud water samples. Cloud samples from two events strongly impacted by biomass burning (19 June (BB-1) and 20 June (BB-2)) are identified with squares and triangles. Samples from other summer cloud events not as strongly influenced by biomass burning (labeled as NBB) are shown as circles. A strong correlation ($R^2 = 0.73$) is observed between TOC and sulfate concentrations in these samples, which come from 18 separate cloud interception events.

the need for scanning across wavelengths or mass-to-charge ratios. Prior to analysis, the TOFMS instrument was tuned and calibrated using a standard ESI-L Low Concentration Tuning Mix (Agilent Technologies). The instrument was calibrated in the low-mass range $m/z < 1700$ using six ions from the calibration mixture with masses of 112.985587, 301.998139, 601.978977, 1033.988109, 1333.968947, and 1633.949786 Da in negative mode, and 118.086255, 322.048121, 622.02896, 922.009798, 1221.990637, and 1521.971475 Da in positive mode. External mass calibration was not used during the analytical run; however, mass shift during the run was insignificant (<1.5 ppm) as confirmed by monitoring the mass of an impurity ion.

[11] A Kinetex 100×3 mm C18 column with 2.6 µm particle size (Phenomenex) was used for chromatographic separation. This chromatographic separation is based on polarity; highly polar compounds elute quickly, while less polar molecules interact more strongly with the stationary phase and elute at longer times. The injection volume was 15 µL and the flow rate 0.5 mL/min. Gradient separation was used with 0.01% of formic acid in water and methanol. The methanol concentration was 20% at the beginning of the run. After 1 min, the methanol concentration was changed linearly to reach 80% at 10 min and was held at 80% for another 5 min.

[12] The combination of liquid chromatography with both online absorbance and MS detection permits direct identification of compounds in cloud water associated with strong absorbance in the near UV and visible. More than 90% of the time, observed absorbance peaks in cloud water UV/Vis chromatograms exhibited a corresponding ion current peak in MS chromatograms. The high-resolution, accurate mass spectra from the ToF-MS allowed determination of the elemental composition of the detected ions. Measured UV/Vis absorbance spectra for these compounds were compared with reference spectra when available.

[13] The composition of nonvolatile water soluble organic carbon in filtered cloud water was also analyzed with an Aerodyne high-resolution Aerosol Mass Spectrometer (AMS). Cloud water samples were atomized, dried with a diffusion drier, and then introduced to the AMS. Detailed procedures for the AMS analysis of liquid samples are given in *Sun et al.* [2010].

3. Results and Discussion

[14] Figures 1a and 1b show photographs of filtered and unfiltered samples of Mt. Tai cloud water collected between 6 and 8 AM (all times local) on 19 June. The unfiltered samples are obviously dark, presumably due to suspended BC, but after filtering through a 0.2 µm pore size filter to remove suspended particles, the samples have an obvious yellow color. As discussed below, these samples were collected from clouds strongly impacted by biomass burning emissions.

3.1. The Composition of Biomass Burning-Impacted Cloud Samples

[15] The relationship between TOC and sulfate concentrations for all Mt. Tai bulk cloud water samples (105 samples from 18 separate cloud interception events) collected during the summer field campaign is shown in Figure 2. Most of the samples exhibit a rather strong ($R^2 = 0.73$) correlation between cloud water TOC and sulfate concentrations. For several samples, the ratio of TOC to sulfate is significantly higher than the typical ratio observed in other cloud water samples collected throughout the summer campaign. The high TOC/sulfate ratio points represent two consecutive sets of samples that were collected between 2:00 and 8:00 AM on 19 June and between 2:00 and 8:15 AM on 20 June. Concentrations of water soluble K^+, one marker for biomass burning [*Ma et al.*, 2003], were significantly elevated in cloud water samples from these two events. The average concentration (± one std dev) of potassium ion observed during the event on 19 June was 10.3 ± 4.8 mg/L and on 20 June was 7.3 ± 2.9 mg/L, higher than the 2.9 ±3.5 mg/L average for summer 2008 Mt. Tai cloud water samples. The ion peak at *m/z* 60 (mainly $C_2H_4O_2^+$) in the AMS mass spectrum of atomized cloud water, another biomass burning marker derived from the fragmentation in the AMS of levoglucosan and other structurally similar molecules derived from combustion of cellulose [*Schneider et al.*, 2006; *Alfarra et al.*, 2007; *Lee et al.*, 2010], was also found to be elevated in these 19 and 20 June cloud samples. The fraction of *m/z* 60 in 19 June samples (0.78%) is much higher than that observed (~0.12%) in the absence of strong biomass burning impact. Two-day back trajectories calculated using NOAA's Hybrid Single-Particle Lagrangian Integrated Trajectory (HYSPLIT) model (shown in Figure 1S in the supplement) (R. R. Draxler and G. D. Rolph, Model access via NOAA ARL READY Website, 2012, http://ready.arl.noaa.gov/HYSPLIT.php, NOAA Air, Resource Laboratory, Silver Spring, MD) further confirmed that the 19 and 20 June air masses sampled at Mt. Tai crossed regions to the southwest with significant agricultural burning indicated by numerous MODIS fire counts (see Figure 2S). The most heavily impacted biomass burning event occurred from 2:00 to 8:00 am on 19 June (referred to as BB-1) with the somewhat less impacted 20 June event labeled as BB-2.

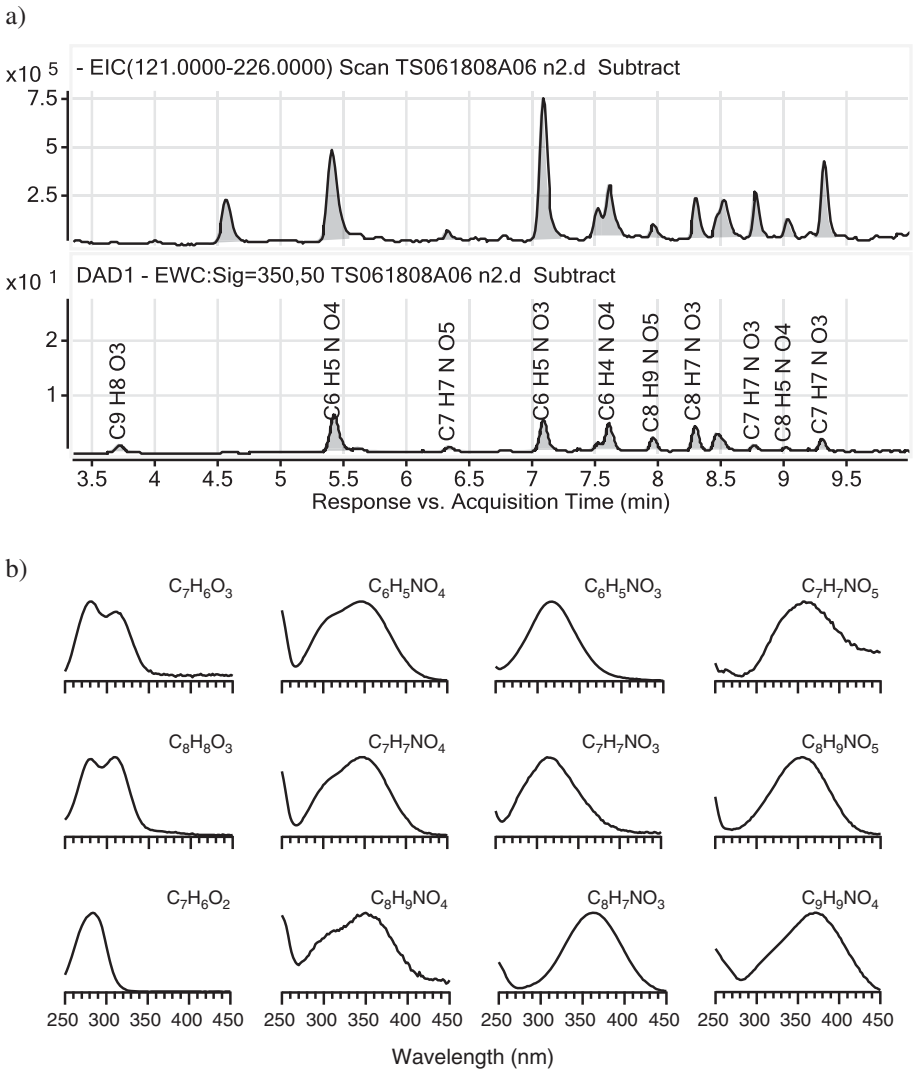

Figure 3. (a) MS, Extracted ion chromatogram (EIC) and UV/Vis diode array detector chromatogram (DAD1) for the cloud water sample collected during the biomass burning-impacted event on 19 June 2008 (TS061808A06). The mass spectrum was acquired using negative mode electrospray ionization. (b) Extracted UV/Vis spectra for selected peaks with assigned elemental formulae.

[16] The average concentration of TOC in cloud water during BB-1 was 100.6 ppmC, approximately eight times higher than typical values observed in summertime Mt. Tai cloud water in the absence of biomass burning, indicating the strong influence that agricultural burning has on cloud organic content. Elevated concentrations of K^+ and Cl^- were also observed in these samples; however, no large impact was observed on cloud water concentrations of sulfate, nitrate, and ammonium. Recent studies from the Fire Laboratory at Missoula Experiments show that the most abundant component emitted from the combustion of most biofuels is carbonaceous material. Cl^- and K^+ are also abundant in smoke emitted from biomass burning (accounting for $40 \pm 14\%$ and $22 \pm 8\%$, respectively, of measured water soluble ion content), while sulfate and nitrate appear to be only minor emissions for most biofuel combustion [*McMeeking et al*., 2009; *Levin et al*., 2010].

3.2. Speciation of BrC in Cloud Water

[17] Figure 3 presents the MS and UV/Vis detector signals for analysis of a cloud water sample collected during the

Table 1. Elemental Formulae Assigned to the Species Responsible for Major Peaks in the UV/Vis Chromatogram

RT, min	Formula	Area, AU	Compound	Reference
2.9	C7 H6 O3	1.46	3,4-Dihydroxy benzaldehyde	[*Láng*, 1975]
3.1	C6 H5 N O5	1.00		
3.7	C9 H8 O3	7.31		
5.4	C6 H5 N O4	33.65	4-Nitrocatechol	[*Cornard et al*., 2005]
6.3	C7 H7 N O5	4.41		
6.8	C8 H7 N O5	1.34		
7.1	C6 H5 N O3	26.70	4-Nitrophenol	standard
7.6	C7 H7 N O4	25.72		
7.9	C8 H9 N O5	8.64		
8.3	C8 H7 N O3	16.14		
8.5	C9 H9 N O4	16.79		
8.7	C7 H7 N O3	3.75	3-Methyl-4-nitrophenol	[*Preiss et al*., 2009]
9.0	C8 H9 N O4	2.60		
9.3	C7 H7 N O3	7.00	2-Methyl-4-nitrophenol	[*Preiss et al*., 2009]
10.1	C8 H9 N O3	2.23		
10.5	C8 H9 N O3	0.53		

Table 2. Concentrations of 4-Nitrophenol Measured in Selected Cloud Water and Aerosol Samples and Corresponding Absorption[a]

Date/Time	Sample Type	4-Nitrophenol Aqueous Conc. (μM)	4-Nitrophenol Air Equivalent Conc. (ng/m^3)	300–400 nm Abs Arbitrary Units	Conditions
6/17 0:00–2:00	LF	0.021	1.060	54	NBB
6/17 0:00–2:00	SF	0.002	0.057	51	NBB
6/19 3:00–4:00	LF	15.1	380	3853	BB
6/19 3:00–4:00	SF	14.5	634	5471	BB
6/19 4:00–6:00	LF	6.7	160	1498	BB
6/19 4:00–6:00	SF	8.1	237	3044	BB
6/20 3:30–5:00	LF	2.2	35	644	BB
6/20 3:30–5:00	SF	3.1	80	790	BB
4/20 0:00–1:00	Bulk	0.001	0.058	34	NBB
4/9 14:00–16:00	Bulk	0.004	0.139	56	NBB
6/19 08:00 – 6/19 18:00	Aerosol	0.014	1.72		BB
6/19 18:00 – 6/20 08:17	Aerosol	0.036	3.00		BB
6/20 08:17 – 6/20 16:45	Aerosol	0.008	1.14		BB
6/20 16:45 – 6/21 08:00	Aerosol	0.024	1.93		BB
6/21 08:00 – 6/22 08:00	Aerosol	0.017	0.85		BB

[a]Samples marked as LF and SF are large and small droplet fraction samples collected by sf-CASCC; samples marked as Bulk are bulk samples collected by CASCC, BB are samples impacted by biomass burning, and NBB are not impacted.

BB-1 event. The absorbance chromatogram shows absorption between 300 and 400 nm, and the MS chromatogram shows total ion counts in the *m/z* range between 60 and 400 Daltons. Almost every peak in the absorbance chromatogram has a corresponding peak in the MS chromatogram (except the one with a retention time (RT) of 3.7 min). Fortunately, the chromatographic separation is sufficient such that we generally observe only one major compound in the MS during each absorbance peak. The accurate mass measurements of the ToF-MS allow determination of an elemental formula for each absorbing compound peak also observed in the MS chromatogram. A list of these peaks with assigned elemental formulae is shown in Table 1. Corresponding UV spectra for these compounds are shown in Figure 3b.

[18] The majority of assigned formulas contain one nitrogen atom and at least three oxygen atoms, suggesting nitro compounds. The presence of oxidized forms of nitrogen is also supported by the detection of these compounds in the negative ion mode of the MS. The absorbance spectrum of the peak that elutes at 7.1 min with assigned elemental formula $C_6H_5NO_3$ was compared with available standards and was found to match the spectrum for 4-nitrophenol. A number of other measured UV/Vis spectra were compared with spectra available in the literature. As shown in Table 1, 4NC (RT = 5.4 min), 2-methyl-4-nitrophenol (RT = 8.75 min), and 3,4-dihydroxy benzaldehyde were identified through matching elemental formulae and absorbance spectra. The compound $C_7H_7NO_4$ at RT 7.7 min has a UV/Vis spectrum very close to the spectrum of 4NC ($C_6H_5NO_4$). It is known that substitution of the methyl group does not change absorbance spectra of aromatic compounds significantly [*Perkampus*, 1992]. In addition, its mass spectrum shows a second peak with an assigned formula of $C_6H_4NO_4$. The odd number of electrons suggests that this peak is produced by the loss of a methyl group due to fragmentation in the mass spectrometer and not a co-eluting compound. Therefore, this compound is likely to be methyl-4NC. 4-nitrophenol, 4NC, and methyl nitrocatechols were also found in $PM_{2.5}$ aerosols affected by biomass burning [*Claeys et al.*, 2012; *Kitanovski et al.*, 2012a, 2012b]. These compounds were also detected in fine aerosol from Los Angeles not impacted by biomass burning [*Zhang et al.*, 2011, 2013] but account for only 4% of light absorption at 365 nm.

[19] A number of nitrophenols have been found in precipitation in previous studies. In precipitation samples collected in Hanover, Germany [*Alber et al.*, 1989; *Böhm et al.*, 1989], a set of nitrophenols was identified, including nitrophenols, methyl nitrophenols, and dinitrophenols. Nitrophenols have also been observed in fog water in California [*Collett et al.*, 1999] and in cloud water and fog water collected in Germany [*Richartz et al.*, 1990; *Lüttke et al.*, 1999]. Biomass burning is known to be a source of nitrophenols, but the concentration of nitrophenols found in cloud water and rain is much higher than might be explained by direct emission. Nitrophenols can be formed in the atmosphere through gas phase and aqueous phase chemistry. The mechanism of nitrophenol formation in the atmosphere is discussed in detail in the review article by *Harrison et al.* [2005].

[20] The acidity of the BB affected cloud samples was in the pH range 3–3.5, which might have aided nitrophenol formation in aqueous phase. A higher rate of photonitration of phenol in aqueous phase was found at lower pH [*Vione et al.*, 2001]. Similar concentrations of 4-nitrophenol were found in cloud and fog water in Germany, France and the UK [*Harrison et al.*, 2005] A strong yellow/brown color of high pH fog samples was also found previously in urban

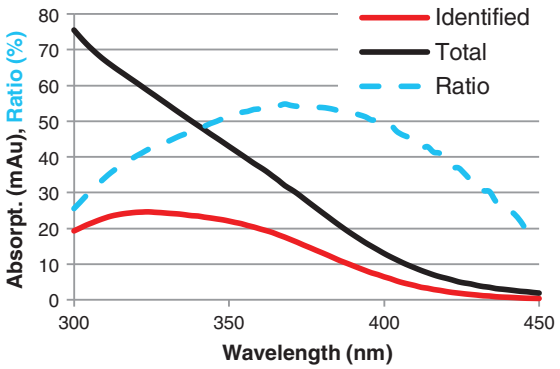

Figure 4. Total absorption, absorption from identified compounds, and the ratio of identified/total absorption vs. wavelength.

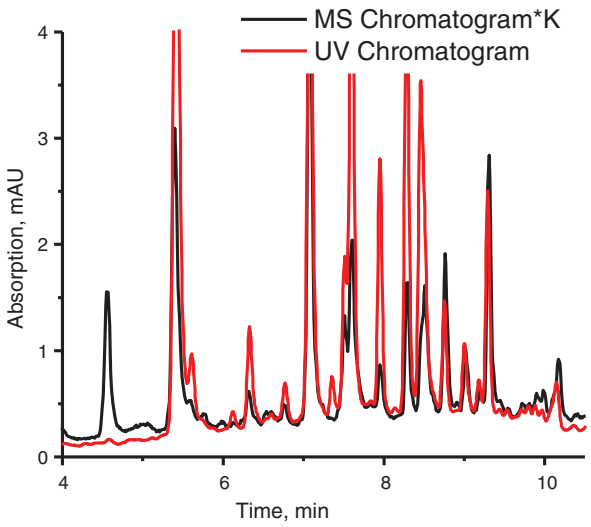

Figure 5. UV/Vis chromatogram and MS chromatogram multiplied by average ratio (K) of the MS to absorbance detector responses.

radiation fogs impacted by residential wood burning in Fresno, California [*Collett et al*., 1999], and thus its occurrence is not limited to low pH or other conditions specific to Mt. Tai. NO_x levels in eastern China are comparable to NO_x levels in Europe and the eastern US [*Miyazaki et al*., 2012]. It is not clear, however, that a high regional NO_x concentration is essential for nitro-aromatic production, given that biomass burning itself is a significant source of NO_x emission [*Zhang et al*., 2003; *Koppmann et al*., 2005; *McMeeking et al*., 2009]. In aerosol samples from Budapest, K-puszta (Europe), and BB-impacted aerosol samples from Brazil, the highest concentration of 4-nitrophenol was found in the samples from Brazil [*Claeys et al*., 2012] where the background NO_x level tends to be low.

[21] A commercial 4-nitrophenol standard was used to calibrate instrument response and measure 4-nitrophenol concentrations in the Mt. Tai samples. The concentrations of 4-nitrophenol in a few samples of Mt. Tai summer 2008 cloud water and aerosol are presented in Table 2. Air equivalent concentrations (the cloud water concentration multiplied by the cloud water LWC to yield mass of compound per volume of air) are presented for the cloud samples to facilitate comparisons to the aerosol concentrations. The cloud water 4-nitrophenol equivalent concentration was 1 µg/m^3 during the peak TOC concentration between 3 and 4 AM on 19 June. It dropped to 400 ng/m^3 over the next 2 h. The cloud water 4-nitrophenol air equivalent concentration was approximately 116 ng/m^3 during the second BB impact event on 20 June. In the absence of biomass burning impact, the 4-nitrophenol concentration was much lower, being 1.1 ng/m^3 on 17 June. In addition, the concentration of the 4-nitrophenol found in aerosol samples even a few hours after biomass burning impact was found to be low, around 1.7 ng/m^3. While cloud scavenging of aerosol particles can be an important contributor to cloud water concentrations of many organic species, the much higher 4-nitrophenol concentrations observed in cloud water support uptake from the gas phase as a likely dominant process. The Henry's law coefficient for 4-nitrophenol was estimated to be around 7.6×10^4 mol/kg *atm at 288 °K [*Guo and Brimblecombe*, 2007]. They estimate that one third to two thirds of 4-nitrophenol will partition to cloud droplets at LWC of 0.2–1.0 g/m^3.

[22] Table 2 shows that short wavelength (300–400 nm) absorbance of the cloud water samples was significantly higher (one to two orders of magnitude) during BB impact events. The change in cloud water absorption due to BB influence is also illustrated in Figure 3S, which compares two UV/Vis absorbance spectra of cloud water samples collected before and during BB impact as well as the absorbance chromatogram measured as these samples were analyzed by LC. The measured cloud water absorption correlates well with cloud water 4-nitrophenol concentrations ($R^2 = 0.93$). The summed absorption by all 16 identified peaks and the total measured absorption over the wavelength range 300–400 nm are shown in Figure 4. This fraction is approximately 26% at 300 nm, grows to 55% at 370 nm, and then drops to 20% at 450 nm. The total area of the 16 peaks from Table 1 accounts for 48% of the overall peak area of the absorbance chromatogram. The absorption chromatogram

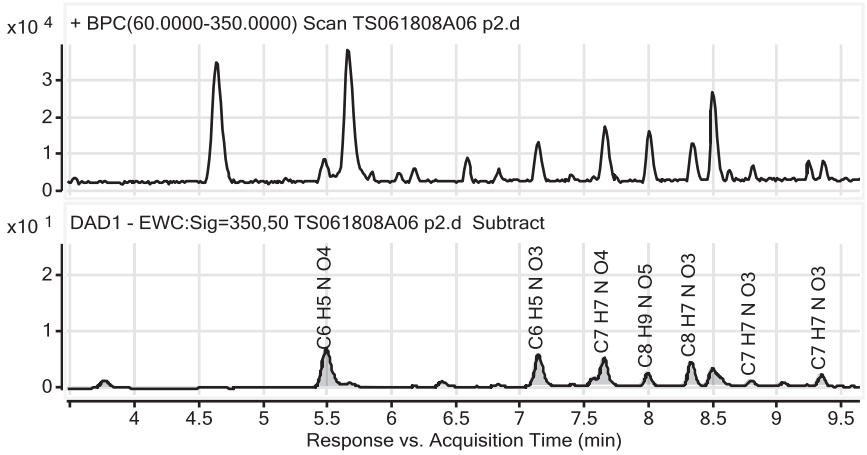

Figure 6. MS, extracted ion chromatogram (EIC), and UV/Vis detector chromatogram (DAD1) for a cloud water sample collected during BB event on 19 June 2008. The mass spectrum was acquired using positive mode electrospray ionization.

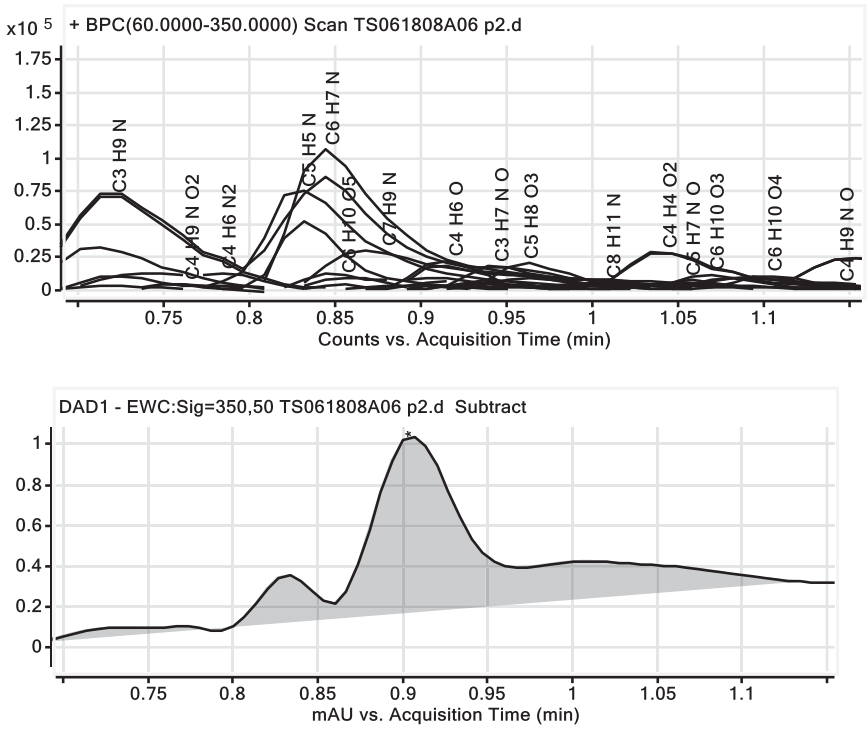

Figure 7. MS, Extracted ion chromatogram (EIC) and UV/Vis detector chromatogram (DAD1) for the same 19 June 2008 cloud water sample zoomed to the first minute. The mass spectrum was acquired using positive mode electrospray ionization. There is no obvious correlation between MS and absorbance detector signals. The MS chromatogram was time corrected to account for the time needed for the sample to pass between the UV/Vis and MS detectors.

can be used to determine the imaginary part of the refractive index needed for radiative transfer modeling if the concentration of the corresponding compounds can be measured using standards or otherwise evaluated.

[23] Figure 4S shows absorption spectra of the cloud water sample collected at the beginning of the BB event before and after filtering. At wavelengths longer than 450 nm, absorption is dominated by nonsoluble material (mostly elemental or BC), while at shorter wavelengths, absorption due to dissolved compounds is more significant. At 300 nm, 80% of the total absorption is due to BrC.

3.3. Other Compounds

[24] Table 1S shows elemental formulas for all MS peaks with intensities higher than 2000 counts. This threshold was chosen because for smaller peaks unambiguous determination of the elemental composition is difficult. There are two distinct groups of compounds. The first group consists of 40 compounds that elute in the first 2.5 min. The number of carbon atoms for compounds in this group, with two exceptions, is between 3 and 6, the double bond equivalent (DBE) is between 1 and 3, and the O/C ratio is between 0.5 and 1. The fraction of measured (300–400 nm) absorbance during the first 2.5 min is approximately 7%. The second group of compounds consists of 65 compounds that elute between 2.5 and 11 min. They have between six and nine carbon atoms and DBE between 5 and 7, indicating that most likely they are aromatic. Forty-six of the 65 compounds in this group contain one or two nitrogen atoms, consistent with a high abundance of nitrogenated species detected in previous studies of fog and precipitation samples [*Altieri et al*., 2009; *Mazzoleni et al*., 2010]. The fraction of total measured (300–400 nm) absorbance in this part of the chromatogram (RT = 2.5 to 11 min) is approximately 92%.

3.4. Baseline Absorption

[25] Clear, distinguishable peaks on the absorbance chromatogram, which can be easily correlated with peaks on the corresponding MS chromatogram, sum up to approximately half of the total absorbance chromatogram area. All of these clearly identifiable peaks eluted after 2.5 min; at shorter RTs, peaks were not resolved in both chromatograms. Due to co-elution of a number of ions in the MS chromatogram, it was hard to assign the absorbance peak to a single ion. The rest of the absorption is due to small and overlapping peaks, and, therefore, it is difficult to assign particular MS ions to them. If we assume that, on average, both absorbance and MS detector responses for the 65 compounds from the second group are similar to the 16 compounds included in Table 1, we can estimate the overall contribution from the 65 compounds to the total absorbance from the MS peak heights. We calculated an average response factor, K, for the 16 compounds from Table 1 as the average ratio of the absorbance peak intensity to the MS peak intensity. Applying this average response factor $K = 1.28*10^{-5} \pm 0.76*10^{-5}$ (mAu s/counts) (± one standard deviation) to the other compounds suggests that, together, these 65 compounds with intensities higher than 2000 counts (including the 16 compounds in Table 1) can explain approximately two thirds (±10%) of the total sample absorption. While this estimate

relies on the assumption that the average detector response ratio of the larger compound group is approximately represented by the subset of 16 clearly isolated compounds, it does give a useful first estimate of the possible contributions of the larger group of compounds to measured cloud water absorbance. Most likely, compounds that yielded intensities lower than 2000 counts in the MS detector (compounds with low abundance and/or compounds that did not yield significant response in the negative ion detection mode with electrospray) account for most of the rest of the absorption.

[26] Figure 5 presents two chromatograms: absorption and total ion current for *m/z* between 121 and 226 Daltons multiplied by K. Corresponding blanks were subtracted from both the absorbance and MS chromatograms. The integration range 121–226 Daltons was chosen to cover the range from lowest to highest masses in Table 1S. Baselines of both the modified MS and absorbance chromatograms closely followed each other, suggesting that the ions detected by mass spectrometry are sufficient to explain all the measured absorbance. The assumption behind this conclusion is that the absorbance and mass spectral detection responses of ions with intensities less than 2000 counts are on average approximately the same as those for ions with intensities exceeding 2000 counts, which assumes their structural similarity. Unfortunately, electrospray ionization mass spectrometry is not sensitive to unfunctionalized aromatic hydrocarbons, and PAH still can contribute to the total UV absorption. Their contribution, however, seems to be small. There is only one absorbance peak without a corresponding MS peak.

3.5. Positive Mode MS Analysis

[27] Compounds detected in positive mode ESI MS also fall into two groups: those that elute in the first 2.5 min and compounds that elute after 2.5 min. The second group of compounds is similar to the compounds detected in negative ion mode as illustrated in Figure 6. Formula assignment for absorbing peaks based on positive mode mass spectra yields the same result as assignments made using negative ion mode detection. By contrast, a number of nitrogen-containing compounds that elute in the first 1.5 min are detected only by positive ion MS. These compounds are presented in Table 2S and shown in Figure 7. They have at most one oxygen atom and one or two nitrogen atoms, suggesting that they are amines and imidazoles. At the eluent pH of approximately 3, these compounds are protonated and will elute quickly from the separation column. Protonated amines have absorption spectra shifted to shorter wavelengths than their neutral forms. Since the Mt. Tai cloud water pH was in the range 3–4 [*Shen et al*., 2012], these compounds should also be protonated in the cloud drops. Accordingly, the absorbance spectra measured in our analysis should reflect the absorption behavior of these species in the clouds. There is no apparent correlation between the absorbance and MS chromatograms in this early time segment. Based on our measurements, amines and imidazoles in the cloud water are estimated to contribute no more than 3% of the total 300–400 nm absorption.

4. Conclusions

[28] Cloud water impacted by agricultural biomass burning was found to contain substantial amounts of BrC. Analysis of the cloud water by liquid chromatography with simultaneous mass spectrometric and absorbance detection provided an opportunity to determine the elemental composition of major chemical solutes that absorb strongly in the UV and short wavelength visible. This approach was used to determine the composition of the 16 strongest absorbers in collected cloud samples. The most important light-absorbing species were nitrophenol derivatives and aromatic carbonyls. Electrospray ionization mass spectrometry is not sensitive to nonfunctionalized aromatic hydrocarbons and PAH that can contribute to total sample absorption. Their contribution, if any, however, seems to be small. Only one absorbance peak was observed without a corresponding MS signature. Absorbance contributions by reduced nitrogen species, while not individually resolved, also appear to comprise less than a few percent of total observed absorbance in the 300–400 nm wavelength range. Total sample absorbance and concentrations of nitrated organics were considerably lower in the absence of biomass burning impact.

[29] This work represents some of the first quantitative measurements of the contributions of individual compounds to light absorption in the 300–400 nm range in the atmospheric aqueous phase. There are several recent studies that examine the BrC constituents in PM2.5 aerosols from photochemical smog events [*Zhang et al*., 2011, 2013] and in biomass burning [*Claeys et al*., 2012]. These analyses were completed on aqueous cloud water samples. Aerosol samples are generally easier to obtain, suggesting future analyses should be extended to more widely available aerosol extracts. Such an effort should include an assessment of whether the absorbance characteristics of compounds of interest are altered by their aqueous dissolution. Future efforts should also quantify the influence of BrC contained in biomass burning-impacted clouds, like those sampled at Mt. Tai, on atmospheric radiative transfer.

[30] **Acknowledgments.** This work was supported by the National Science Foundation (AGS-0711102 and AGS-0521643) and by the U.S. Joint Fire Science Program. We thank Jia Guo, Wenxing Wang, and Tingli Sun at Shandong University for their assistance in the Mt. Tai cloud sampling campaign that collected the samples analyzed in this project.

References

Alber, M., H. B. Böhm, J. Brodesser, J. Feltes, K. Levsen, and H. F. Schöler (1989), Determination of nitrophenols in rain and snow, *Fresenius J. Anal. Chem.*, *334*(6), 540–545, doi:10.1007/BF00483573.

Alexander, D. T. L., P. A. Crozier, and J. R. Anderson (2008), Brown carbon spheres in East Asian outflow and their optical properties, *Science*, *321*(5890), 833–836, doi:10.1126/science.1155296.

Alfarra, M. R., A. S. H. Prevot, S. Szidat, J. Sandradewi, S. Weimer, V. A. Lanz, D. Schreiber, M. Mohr, and U. Baltensperger (2007), Identification of the mass spectral signature of organic aerosols from wood burning emissions, *Environ. Sci. Technol.*, *41*(16), 5770–5777, doi:10.1021/ES062289B.

Altieri, K. E., B. J. Turpin, and S. P. Seitzinger (2009), Oligomers, organosulfates, and nitrooxy organosulfates in rainwater identified by ultra-high resolution electrospray ionization FT-ICR mass spectrometry, *Atmos. Chem. Phys.*, *9*(7), 2533–2542, doi:10.5194/ACP-9-2533-2009.

Andreae, M. O., and A. Gelencsér (2006), Black carbon or brown carbon? The nature of light-absorbing carbonaceous aerosols, *Atmos. Chem. Phys.*, *6*(10), 3131–3148, doi:10.5194/ACP-6-3131-2006.

Arola, A., G. Schuster, G. Myhre, S. Kazadzis, S. Dey, and S. N. Tripathi (2011), Inferring absorbing organic carbon content from AERONET data, *Atmos. Chem. Phys.*, *11*(1), 215–225, doi:10.5194/ACP-11-215-2011.

Barnard, J. C., R. Volkamer, and E. I. Kassianov (2008), Estimation of the mass absorption cross section of the organic carbon component of aerosols in the Mexico City Metropolitan Area, *Atmos. Chem. Phys.*, *8*(22), 6665–6679, doi:10.5194/ACP-8-6665-2008.

Bergstrom, R. W., P. B. Russell, and P. Hignett (2002), Wavelength dependence of the absorption of black carbon particles: Predictions and results from the TARFOX experiment and implications for the aerosol single scattering albedo, *J. Atmos. Sci.*, *59*(3), 567–577, doi:10.1175/1520-0469(2002).

Bergstrom, R. W., P. Pilewskie, P. B. Russell, J. Redemann, T. C. Bond, P. K. Quinn, and B. Sierau (2007), Spectral absorption properties of atmospheric aerosols, *Atmos. Chem. Phys.*, *7*(23), 5937–5943, doi:10.5194/ACP-7-5937-2007.

Böhm, H. B., J. Feltes, D. Volmer, and K. Levsen (1989), Identification of nitrophenols in rain-water by high-performance liquid chromatography with photodiode array detection, *J. Chromatogr. A*, *478*, 399–407, doi:10.1016/0021-9673(89)90041-1.

Bond, T. C., and R. W. Bergstrom (2006), Light absorption by carbonaceous particles: An investigative review, *Aerosol Sci. Technol.*, *40*(1), 27–67, doi:10.1080/02786820500421521.

Bones, D. L., D. K. Henricksen, S. A. Mang, M. Gonsior, A. P. Bateman, T. B. Nguyen, W. J. Cooper, and S. A. Nizkorodov (2010), Appearance of strong absorbers and fluorophores in limonene-O3 secondary organic aerosol due to NH4 + -mediated chemical aging over long time scales, *J. Geophys. Res.*, *115*, D05203, doi:10.1029/2009JD012864.

Chakrabarty, R. K., H. Moosmüller, L.-W. A. Chen, K. Lewis, W. P. Arnott, C. Mazzoleni, M. K. Dubey, C. E. Wold, W. M. Hao, and S. M. Kreidenweis (2010), Brown carbon in tar balls from smoldering biomass combustion, *Atmos. Chem. Phys.*, *10*(13), 6363–6370, doi:10.5194/ACP-10-6363-2010.

Chang, J. L., and J. E. Thompson (2010), Characterization of colored products formed during irradiation of aqueous solutions containing H2O2 and phenolic compounds, *Atmos. Environ.*, *44*(4), 541–551, doi:10.1016/j.atmosenv.2009.10.042.

Chen, Y., and T. C. Bond (2010), Light absorption by organic carbon from wood combustion, *Atmos. Chem. Phys.*, *10*(4), 1773–1787, doi:10.5194/ACP-10-1773-2010.

Chuang, P. Y., R. M. Duvall, M. S. Bae, A. Jefferson, J. J. Schauer, H. Yang, J. Z. Yu, and J. Kim (2003), Observations of elemental carbon and absorption during ACE-Asia and implications for aerosol radiative properties and climate forcing, *J. Geophys. Res.*, *108*(D23), 8634, doi:10.1029/2002JD003254.

Claeys, M., R. Vermeylen, F. Yasmeen, Y. Gómez-González, X. Chi, W. Maenhaut, T. Mészáros, and I. Salma (2012), Chemical characterisation of humic-like substances from urban, rural and tropical biomass burning environments using liquid chromatography with UV/vis photodiode array detection and electrospray ionisation mass spectrometry, *Environ. Chem.*, *9*(3), 273–284.

Clarke, A., et al. (2007), Biomass burning and pollution aerosol over North America: Organic components and their influence on spectral optical properties and humidification response, *J. Geophys. Res.*, *112*, D12S18, doi:10.1029/2006JD007777.

Collett, J. L., Jr., K. J. Hoag, X. Rao, and S. N. Pandis (1999), Internal acid buffering in San Joaquin Valley fog drops and its influence on aerosol processing, *Atmos. Environ.*, *33*(29), 4833–4847, doi:10.1016/S1352-2310(99)00221-6.

Cooke, W. F., C. Liousse, H. Cachier, and J. Feichter (1999), Construction of a 1° × 1° fossil fuel emission data set for carbonaceous aerosol and implementation and radiative impact in the ECHAM4 model, *J. Geophys. Res.*, *104*(D18), 22,137–22,162, doi:10.1029/1999JD900187.

Cornard, J.-P., Rasmiwetti, and J.-C. Merlin (2005), Molecular structure and spectroscopic properties of 4-nitrocatechol at different pH: UV–visible, Raman, DFT and TD-DFT calculations, *Chem. Phys.*, *309*(2–3), 239–249, doi:10.1016/j.chemphys.2004.09.020.

Demoz, B. B., J. L. Collett Jr., and B. C. Daube Jr. (1996), On the Caltech active strand cloudwater collectors, *Atmos. Res.*, *41*(1), 47–62, doi:10.1016/0169-8095(95)00044-5.

Feng, Y., V. Ramanathan, and V. R. Kotamarthi (2013), Brown carbon: A significant atmospheric absorber of solar radiation?, *Atmos. Chem. Phys. Discuss.*, *13*(1), 2795–2833, doi:10.5194/ACPD-13-2795-2013.

Formenti, P., W. Elbert, W. Maenhaut, J. Haywood, S. Osborne, and M. O. Andreae (2003), Inorganic and carbonaceous aerosols during the Southern African Regional Science Initiative (SAFARI 2000) experiment: Chemical characteristics, physical properties, and emission data for smoke from African biomass burning, *J. Geophys. Res.*, *108*(D13), 8488, doi:10.1029/2002JD002408.

Guo, X. X., and P. Brimblecombe (2007), Henry's law constants of phenol and mononitrophenols in water and aqueous sulfuric acid, *Chemosphere*, *68*(3), 436–444, doi:10.1016/j.chemosphere.2007.01.011.

Hansen, A. D. A., H. Rosen, and T. Novakov (1984), The aethalometer — An instrument for the real-time measurement of optical absorption by aerosol particles, *Sci. Total Environ.*, *36*, 191–196, doi:10.1016/0048-9697(84)90265-1.

Harrison, M. A. J., S. Barra, D. Borghesi, D. Vione, C. Arsene, and R. Iulian Olariu (2005), Nitrated phenols in the atmosphere: A review, *Atmos. Environ.*, *39*(2), 231–248, doi:10.1016/j.atmosenv.2004.09.044.

Hecobian, A., X. Zhang, M. Zheng, N. Frank, E. S. Edgerton, and R. J. Weber (2010), Water-soluble organic aerosol material and the light-absorption characteristics of aqueous extracts measured over the Southeastern United States, *Atmos. Chem. Phys.*, *10*(13), 5965–5977, doi:10.5194/ACP-10-5965-2010.

Hoffer, A., A. Gelencsér, P. Guyon, G. Kiss, O. Schmid, G. P. Frank, P. Artaxo, and M. O. Andreae (2006), Optical properties of humic-like substances (HULIS) in biomass-burning aerosols, *Atmos. Chem. Phys.*, *6*(11), 3563–3570, doi:10.5194/ACP-6-3563-2006.

Jacobson, M. Z. (1999), Isolating nitrated and aromatic aerosols and nitrated aromatic gases as sources of ultraviolet light absorption, *J. Geophys. Res.*, *104*(D3), 3527–3542, doi:10.1029/1998JD100054.

Jaoui, M., E. O. Edney, T. E. Kleindienst, M. Lewandowski, J. H. Offenberg, J. D. Surratt, and J. H. Seinfeld (2008), Formation of secondary organic aerosol from irradiated α-pinene/toluene/NOx mixtures and the effect of isoprene and sulfur dioxide, *J. Geophys. Res.*, *113*, D09303, doi:10.1029/2007JD009426.

Kelly, J. L., D. V. Michelangeli, P. A. Makar, D. R. Hastie, M. Mozurkewich, and J. Auld (2010), Aerosol speciation and mass prediction from toluene oxidation under high NOx conditions, *Atmos. Environ.*, *44*(3), 361–369, doi:10.1016/j.atmosenv.2009.10.035.

Kirchstetter, T. W., T. Novakov, and P. V. Hobbs (2004), Evidence that the spectral dependence of light absorption by aerosols is affected by organic carbon, *J. Geophys. Res.*, *109*, D21208, doi:10.1029/2004JD004999.

Kitanovski, Z., I. Grgić, F. Yasmeen, M. Claeys, and A. Čusak (2012a), Development of a liquid chromatographic method based on ultraviolet–visible and electrospray ionization mass spectrometric detection for the identification of nitrocatechols and related tracers in biomass burning atmospheric organic aerosol, *Rapid Commun. Mass Spectrom.*, *26*(7), 793–804, doi:10.1002/RCM.6170.

Kitanovski, Z., I. Grgić, R. Vermeylen, M. Claeys, and W. Maenhaut (2012b), Liquid chromatography tandem mass spectrometry method for characterization of monoaromatic nitro-compounds in atmospheric particulate matter, *J. Chromatogr. A*, *1268*, 35–43, doi:10.1016/j.chroma.2012.10.021.

Koppmann, R., K. von Czapiewski, and J. S. Reid (2005), A review of biomass burning emissions, Part I: Gaseous emissions of carbon monoxide, methane, volatile organic compounds, and nitrogen containing compounds, *Atmos. Chem. Phys. Discuss.*, *5*(5), 10455–10516, doi:10.5194/ACPD-5-10455-2005.

Láng, L. (1975), *Absorption Spectra in the Ultraviolet and Visible Region*, Academic Press, New York.

Lee, T., et al. (2010), Chemical smoke marker emissions during flaming and smoldering phases of laboratory open burning of wildland fuels, *Aerosol Sci. Technol.*, *44*(9), i–v, doi:10.1080/02786826.2010.499884.

Levin, E. J. T., et al. (2010), Biomass burning smoke aerosol properties measured during Fire Laboratory at Missoula Experiments (FLAME), *J. Geophys. Res.*, *115*, D18210, doi:10.1029/2009JD013601.

Lewis, K., W. P. Arnott, H. Moosmüller, and C. E. Wold (2008), Strong spectral variation of biomass smoke light absorption and single scattering albedo observed with a novel dual-wavelength photoacoustic instrument, *J. Geophys. Res.*, *113*, D16203, doi:10.1029/2007JD009699.

Lukács, H., et al. (2007), Seasonal trends and possible sources of brown carbon based on 2-year aerosol measurements at six sites in Europe, *J. Geophys. Res.*, *112*, D23S18, doi:10.1029/2006JD008151.

Lüttke, J., K. Levsen, K. Acker, W. Wieprecht, and D. Möller (1999), Phenols and nitrated phenols in clouds at Mount Brocken, *Int. J. Environ. Anal. Chem.*, *74*(1-4), 69–89, doi:10.1080/03067319908031417.

Ma, Y., et al. (2003), Characteristics and influence of biosmoke on the fine-particle ionic composition measured in Asian outflow during the Transport and Chemical Evolution Over the Pacific (TRACE-P) experiment, *J. Geophys. Res.*, *108*(D21), 8816, doi:10.1029/2002JD003128.

Mazzoleni, L. R., B. M. Ehrmann, X. Shen, A. G. Marshall, and J. L. Collett (2010), Water-soluble atmospheric organic matter in fog: Exact masses and chemical formula identification by ultrahigh-resolution fourier transform ion cyclotron resonance mass spectrometry, *Environ. Sci. Technol.*, *44*(10), 3690–3697, doi:10.1021/ES903409K.

McMeeking, G. R., et al. (2009), Emissions of trace gases and aerosols during the open combustion of biomass in the laboratory, *J. Geophys. Res.*, *114*, D19210, doi:10.1029/2009JD011836.

Miyazaki, K., H. J. Eskes, and K. Sudo (2012), Global NOx emission estimates derived from an assimilation of OMI tropospheric NO2 columns, *Atmos. Chem. Phys.*, *12*(5), 2263–2288, doi:10.5194/ACP-12-2263-2012.

Moosmüller, H., R. K. Chakrabarty, and W. P. Arnott (2009), Aerosol light absorption and its measurement: A review, *J. Quant. Spectrosc. Radiat. Transfer*, *110*(11), 844–878, doi:10.1016/j.jqsrt.2009.02.035.

Moosmüller, H., R. K. Chakrabarty, K. M. Ehlers, and W. P. Arnott (2011), Absorption Ångström coefficient, brown carbon, and aerosols: Basic concepts, bulk matter, and spherical particles, *Atmos. Chem. Phys.*, *11*(3), 1217–1225, doi:10.5194/ACP-11-1217-2011.

Penner, J. E., H. Eddleman, and T. Novakov (1993), Towards the development of a global inventory for black carbon emissions, *Atmos. Environ. Part A*, *27*(8), 1277–1295, doi:10.1016/0960-1686(93)90255-W.

Perkampus, H.-H. (1992), *UV-VIS Atlas of Organic Compounds*, VCH, Weinheim, New York.

Preiss, A., A. Bauer, H.-M. Berstermann, S. Gerling, R. Haas, A. Joos, A. Lehmann, L. Schmalz, and K. Steinbach (2009), Advanced high-performance liquid chromatography method for highly polar nitroaromatic compounds in ground water samples from ammunition waste sites, *J. Chromatogr. A*, *1216*(25), 4968–4975, doi:10.1016/j.chroma.2009.04.055.

Ramanathan, V., and G. Carmichael (2008), Global and regional climate changes due to black carbon, *Nat. Geosci.*, *1*(4), 221–227, doi:10.1038/NGEO156.

Richartz, H., A. Reischl, F. Trautner, and O. Hutzinger (1990), Nitrated phenols in fog, *Atmos. Environ. Part A*, *24*(12), 3067–3071, doi:10.1016/0960-1686(90)90485-6.

Rizzo, L. V., A. L. Correia, P. Artaxo, A. S. Procópio, and M. O. Andreae (2011), Spectral dependence of aerosol light absorption over the Amazon Basin, *Atmos. Chem. Phys. Discuss.*, *11*(4), 11547–11577, doi:10.5194/ACPD-11-11547-2011.

Rosen, H., and T. Novakov (1977), Raman scattering and the characterisation of atmospheric aerosol particles, *Nature*, *266*(5604), 708–710, doi:10.1038/266708A0.

Schnaiter, M., H. Horvath, O. Möhler, K.-H. Naumann, H. Saathoff, and O. W. Schöck (2003), UV-VIS-NIR spectral optical properties of soot and soot-containing aerosols, *J. Aerosol Sci.*, *34*(10), 1421–1444, doi:10.1016/S0021-8502(03)00361-6.

Schneider, J., S. Weimer, F. Drewnick, S. Borrmann, G. Helas, P. Gwaze, O. Schmid, M. O. Andreae, and U. Kirchner (2006), Mass spectrometric analysis and aerodynamic properties of various types of combustion-related aerosol particles, *Int. J. Mass Spectrom.*, *258*(1–3), 37–49, doi:10.1016/j.ijms.2006.07.008.

Shapiro, E. L., J. Szprengiel, N. Sareen, C. N. Jen, M. R. Giordano, and V. F. McNeill (2009), Light-absorbing secondary organic material formed by glyoxal in aqueous aerosol mimics, *Atmos. Chem. Phys.*, *9*(7), 2289–2300, doi:10.5194/ACP-9-2289-2009.

Shen, X., et al. (2012), Aqueous phase sulfate production in clouds in eastern China, *Atmos. Environ.*, *62*, 502–511, doi:10.1016/j.atmosenv.2012.07.079.

Sun, Y. L., Q. Zhang, C. Anastasio, and J. Sun (2010), Insights into secondary organic aerosol formed via aqueous-phase reactions of phenolic compounds based on high resolution mass spectrometry, *Atmos. Chem. Phys.*, *10*(10), 4809–4822, doi:10.5194/ACP-10-4809-2010.

Vione, D., V. Maurino, C. Minero, and E. Pelizzetti (2001), Phenol photonitration upon UV irradiation of nitrite in aqueous solution, II: Effects of pH and TiO2, *Chemosphere*, *45*(6-7), 903–910, doi:10.1016/S0045-6535(01)00036-4.

Zhang, R., X. Tie, and D. W. Bond (2003), Impacts of anthropogenic and natural NOx sources over the U.S. on tropospheric chemistry, *Proc. Natl. Acad. Sci. U. S. A.*, *100*(4), 1505–1509, doi:10.1073/PNAS.252763799.

Zhang, X., Y.-H. Lin, J. D. Surratt, P. Zotter, A. S. H. Prévôt, and R. J. Weber (2011), Light-absorbing soluble organic aerosol in Los Angeles and Atlanta: A contrast in secondary organic aerosol, *Geophys. Res. Lett.*, *38*, L21810, doi:10.1029/2011GL049385.

Zhang, X., Y.-H. Lin, J. D. Surratt, and R. J. Weber (2013), Sources, composition and absorption Ångström exponent of light-absorbing organic components in aerosol extracts from the Los Angeles Basin, *Environ. Sci. Technol.*, *47*, 3685–3693, doi:10.1021/ES305047B.

Zhong, M., and M. Jang (2011), Light absorption coefficient measurement of SOA using a UV–Visible spectrometer connected with an integrating sphere, *Atmos. Environ.*, *45*(25), 4263–4271, doi:10.1016/j.atmosenv.2011.04.082.